Energy for Sustainable Development 34 (2016) 54–61

Contents lists available at ScienceDirect

Energy for Sustainable Development

Uncertainty analysis and design guidelines of biomass cookstove thermal efficiency studies

Cameron M. Quist [a], Rory B. Jones [a], Matthew R. Jones [b], Randy S. Lewis [a,*]

[a] Department of Chemical Engineering, Brigham Young University, Provo, UT 84602, USA
[b] Department of Mechanical Engineering, Brigham Young University, Provo, UT 84602, USA

ARTICLE INFO

Article history:
Received 20 July 2015
Revised 23 May 2016
Accepted 13 July 2016
Available online xxxx

Keywords:
Cookstove
Uncertainty
Analysis
Experimental design
Water Boiling Test

ABSTRACT

Many individuals in developing areas use biomass cookstoves for cooking although there are many inherent health hazards. Judging which improved cookstove to use and distinguishing the best one for a given cooking style to mitigate these hazards is challenging. Thermal efficiency (η_{th}) is one assessment parameter of cookstoves that is often used. To compare η_{th} between cookstoves or to assess the effects of a design change on η_{th}, it is important to understand how the uncertainty in η_{th} depends on measurements, input data (equipment uncertainties, literature values, etc.), and test conditions. In this work, measurement and input data uncertainties are quantified with a propagation of uncertainty analysis for a basic brick channel cookstove used in many Peruvian households. This method can be used in any study by using reasonable uncertainty values for that study. Results showed that the four main parameters contributing to 93% of the η_{th} uncertainty were the lower heating values (LHV) of wood and char, the moisture content, and the change in temperature of the water in the pot. Reducing the uncertainty of LHV of unprocessed fuels is the most difficult. If such fuels are used, reporting the LHV value and its associated uncertainty is highly valuable.

Introduction

The hazards of using biomass cookstoves on a daily basis are well documented, including the potential of asthma, cancer, carbon monoxide poisoning, and others (Mueller et al., 2011; Chowdhury, 2012; Abeliotis and Pakula, 2013; Hawley and Volckens, 2013). In addition to the personal risk of using biomass cookstoves, there are significant environmental effects. The pollutants released are greenhouse gas emissions, and the particulate matter can increase global climate change (Bond et al., 2013). Despite these health risks and the environmental damage, those living in developing regions often have no option other than the continued use of biomass to cook and to heat their homes.

Beginning in the mid-1980s, many organizations have made efforts to mitigate the health and environmental hazards by engineering and distributing more efficient, cleaner burning biomass cookstoves (Baldwin, 1987). Improved cookstove designs have ranged from wood burning rocket stoves to cookstoves specializing in the use of farming waste. Assessment of the performance of improved cookstoves has been conducted using the Water Boiling Test (WBT) or a variant thereof (Jetter et al., 2012; Manoj et al., 2013; Bailis et al., 2014; Kshirsagar and Kalamkar, 2014). Two commonly reported values from these tests are the modified combustion efficiency (MCE), often observed above 90%, and the thermal efficiency (η_{th}) which is often shown to be below 50% (Jetter et al., 2012). This work focuses on η_{th}.

Recent efforts to improve η_{th} have involved modeling the heat transfer, in whole or in part, and then improving the cookstove design (Wohlgemuth et al., 2009; Agenbroad, 2010; Andreatta and Wohlgemuth, 2010; MacCarty and Bryden, 2015). However, physical tests are still required for model validation and for comparing η_{th} of cookstoves based on changes to cookstove designs. Usually, the average η_{th} for a number of test replicates (and sometimes standard deviation or confidence interval) is reported in the literature to compare various cookstoves or to assess design changes. To effectively compare η_{th} between cookstoves or to assess the effects of a design change on η_{th}, it is important to understand how the uncertainty in η_{th} depends on measurements, input data (manufacturing specifications, literature values, etc.), and test conditions.

The uncertainty associated with measurements, input data, and test conditions can be a result of uncertainties in the models and input parameters, variability in the equipment used in testing, and random changes in test conditions such as wind speed, ambient temperature, the method in which wood is stacked within or the method in which fuel is fed into the cookstove. Valid, unbiased comparison of cookstove performance can only be made if variations in conditions in which the tests were performed and the uncertainties in measurements and input data are reported. Unfortunately, variations can also occur both with different testers and the same tester (Zube, 2010). Fortunately,

* Corresponding author at: Department of Chemical Engineering, 350 Clyde Building, Brigham Young University, Provo, UT 84602, USA. Tel.: +1 8014227863; fax: +1 8014220151.

E-mail address: randy.lewis@byu.edu (R.S. Lewis).

http://dx.doi.org/10.1016/j.esd.2016.07.001

measurement and input data uncertainties can be quantified with a propagation of uncertainty analysis based upon the equations used to calculate η_{th}. The focus of this work is to address the uncertainty of η_{th} associated with measurements and input data. Although uncertainty of η_{th} associated with various testing conditions is not the focus of this work, it is important to reemphasize the need to report testing conditions to adequately compare η_{th} reported in the literature.

Materials and methods

Testing chamber and cookstove

As shown in Fig. 1A, a cinderblock structure (1.4 m long × 0.8 m wide × 0.7 m high) was built on a rolling metal cart. The cookstove was placed in the cinderblock housing on a 6.4-mm thick metal plate. Underneath the plate was a 10 cm deep container of sand used to imitate an in-home cookstove placed on the ground. The cinderblock housing was topped by a hood through which the exhaust flowed through a fan and a flue at an approximate flow rate of 16 L/min.

The cookstove used for this study simulated a basic channel cookstove used in many Peruvian households in the Piura region. The basic design of this cookstove is simply two small, parallel walls of bricks that are placed far enough from each other to maximize the fire while still holding the cooking pot above the fire. The brick walls used in these experiments were 2.5 bricks high and 2.5 bricks long, which resulted in a wall 14 cm tall by 56 cm long and 10 cm wide. The walls were set approximately 15 cm apart. The effects of three modifications to the channel cookstove on η_{th} were investigated. First, a grate was included by adding one additional layer of bricks (adding an additional 5.5 cm to the height) and placing the grate between the lower and middle layers of brick. The intent of this modification was to reduce heat loss to the ground and to improve the combustion efficiency by increasing airflow into the combustion zone. Second, a pot skirt made of bent metal sheets to conform to the sides of the pot was added to increase heat transfer to the pot (shown in Fig. 1C). Third, the combined effects of the grate and skirt were investigated. The basic cookstove design was tested seven times, the grate addition six times, the skirt addition nine times, and the grate/skirt addition five times.

Experimental protocol

For each test, a 15-L pot (25 cm high, and 25 cm diameter) filled with 2.5 L of water was placed on the cookstove. The temperature of the water was continuously measured using a k-type thermocouple. Douglas fir was cut into uniform sticks (2 cm × 2 cm × 25 cm) for each experiment. The wood was dried in a dehydrator for approximately 24 h before testing to maintain consistency in the moisture content.

Fig. 1. (A) Cookstove testing chamber with a traditional Peruvian brick channel stove resting atop a metal plate. The hood vented to a chimney augmented by a fan that can be seen directly above the apex of the hood. (B) The wood was arranged in a 'log-cabin' configuration made of sticks measuring 2 cm × 2 cm × 13 cm. There were 4 layers of sticks, with each layer containing 2 sticks. (C) Skirt surrounding pot.

The wood moisture content was measured at the beginning of each run using a wood moisture meter (MMD4E The Seeker, General Tools, New York City, NY). For all runs, the moisture content was below the detectable limit of the meter (5%). While using a moisture meter is not the preferred method for determining moisture content in the WBT protocol, it is mentioned as an option and is an inexpensive and fast method. For this study, moisture meter measurement error was used to provide a worse-case scenario as to the contribution of this measurement error to η_{th} analysis.

The WBT was performed during each run to obtain η_{th}. The wood was arranged in a 'log-cabin' configuration at the beginning of each cold start phase as shown in Fig. 1B. For the log-cabin, the sticks were cut in half and four layers of sticks were stacked, with each layer containing two sticks. The cold start is where the cookstove begins at ambient temperature. Newspaper and splintered wood were placed in the center as starter and kindling and the fire was started. At each four minute interval following the start of the fire, an alternating pattern of three wood sticks and then two wood sticks were added to the existing fire until the water boiled. At this point, the fire was extinguished by removal from the cookstove and smothering. The amount of wood and charcoal remaining was measured using a digital scale with an accuracy of ±0.5 g. The charcoal was obtained by both removing the charcoal in the combustion chamber and by shaving off the charcoal from the remaining wood with a file. After the cold start analysis, all charcoal and wood were removed from the cookstove and the process described for the cold start was repeated with a fresh pot again filled with 2.5 L of water. The only difference was that the cookstove was now warm at the beginning of the burn. This phase is called the hot start phase. Once the water boiled in the hot start phase, the fire was extinguished and the remaining wood and charcoal were weighed. Then, additional hot start phases were continued. Only runs involving the hot start phase were analyzed in this work to reduce variability in the analysis.

Calculation of the thermal efficiency, η_{th}

As previously defined (Bailis et al. 2014), η_{th} is the ratio of the energy transferred to the water in the pot (E_{pot}) to the energy available in the fuel (E_{fuel}):

$$\eta_{th} = \frac{E_{pot}}{E_{fuel}} \quad (1)$$

Monitoring the temperature of the water in the pot, measuring the mass of water that evaporated, and determining the amount of wood consumed are some of the key aspects needed to determine η_{th} (Bailis et al., 2014; Poudyal et al., 2015).

The amount of energy transferred to the pot is calculated according to

$$E_{pot} = Cp_w * m_{water,i} * \Delta T + \Delta h_{H2O,fg} * \Delta m_{water} \quad (2)$$

where Cp_w is the specific heat of water, $m_{water,i}$ is the initial mass of water in the pot, ΔT is the final temperature of water minus the initial temperature of water in the pot, $\Delta h_{H2O,fg}$ is the heat of vaporization of saturated water at the ambient pressure (often approximated as the heat of vaporization at $P_{amb} = 1$ atm or $T = 100$ °C), and Δm_{water} is the change in mass of water in the pot. In Eq. (2), the first term accounts for the energy used to heat the water and the second term accounts for the energy used in water evaporation.

The energy in the fuel is approximated as

$$E_{fuel} = f_{cd} * LHV_{wood} \quad (3)$$

where f_{cd} is the equivalent dry weight of wood consumed and LHV_{wood} is the lower heating value of the wood consumed on a dry basis. f_{cd} is a way to group variables for calculating η_{th} and is defined as,

$$f_{cd} = f_{cm} * (1-MC) - f_{cm} * \mathrm{MC} * \mathrm{y} - \frac{LHV_c}{LHV_{wood}} * m_c \quad (4)$$

where f_{cm} is the mass of the fuel consumed during the test including the moisture in the fuel, MC is the initial moisture mass fraction of the wood (g/g), LHV_c is the lower heating value of the charcoal obtained from burning the wood, m_c is the mass of the charcoal remaining, and y is the ratio of energy used to remove moisture from the wood relative to energy available in the dry wood. Specifically,

$$y = \frac{[Cp*(T_{boil} - T_{amb}) + \Delta h_{H2O,fg}]}{LHV_{wood}} \quad (5)$$

where T_{boil} is the boiling temperature of water (based on ambient pressure) and T_{amb} is the ambient temperature during the test. In Eq. (4), the first term describes the energy released from the moisture-free burned wood, the second term describes the energy used to volatilize the moisture in the wood and the third term describes the energy remaining in the charcoal after the test is completed.

Uncertainty of η_{th}

The maximum uncertainty in η_{th}, due to uncertainties in both measurements and input data, is denoted as δ_{th}. The maximum uncertainty in η_{th} was calculated for each experiment based on the propagation of uncertainty (Bethea and Rhinehart, 1991) according to

$$\delta_{th} = \sum_i \left(\left| \frac{\partial \eta_{th}}{\partial x_i} \right| \delta_i \right) \quad (6)$$

Here, x_i represents each measurement and input data parameter in Eqs. (2)–(4) that is used to calculate η_{th} and i is the total number of parameters (see Table 2 for x_i parameters). δ_i is the maximum uncertainty associated with each x_i. Thus, δ_{th} is found by summing the product of δ_i and the partial derivative (or sensitivity) of the thermal efficiency with respect to x_i evaluated at the average value of each x_i.

The fractional contribution, f_i, of each parameter to δ_{th} is defined as

$$f_i = \left| \frac{\partial \eta_{th}}{\partial x_i} \right| \frac{\delta_i}{\delta_{th}} \quad (7)$$

The fractional contribution is useful in determining the relative importance of the uncertainty in each parameter to η_{th}.

In addition to calculating the maximum uncertainty of η_{th}, the propagated standard deviation of η_{th} was also calculated to enable the calculation of confidence intervals for η_{th} based on measured and input data uncertainties. In general, a 99% confidence interval would have a smaller interval than the maximum uncertainty interval since the maximum uncertainty assumes that all uncertainty for each parameter x_i would propagate at the maximum uncertainty. A maximum uncertainty actually occurring is also very unlikely to be observed in practice. The propagated standard deviation (σ_{th}) is calculated according to

$$\sigma_{th} = \sqrt{\sum_i \left(\left| \frac{\partial \eta_{th}}{\partial x_i} \right| \sigma_i \right)^2} \quad (8)$$

where σ_i is the standard deviation of the measured or input data parameter x_i.

A more intriguing form of Eqs. (6)–(8) is obtained by multiplying and dividing the right side of Eq. (6) by η_{th} to obtain:

$$\delta_{th} = \sum_i \left(\left| \frac{\partial \eta_{th}}{\partial x_i} \right| \delta_i \right) = \eta_{th} \sum_i \left(\frac{\left| \frac{\partial \eta_{th}}{\partial x_i} \right| \delta_i}{\eta_{th}} \right) = \eta_{th} \sum_i \O_i \quad (9)$$

where ϕ_i is a new variable that represents the contribution of each parameter x_i to δ_{th}. Here, the summation of ϕ_i provides information on the value of δ_{th} relative to η_{th}. Similarly, substituting the definition of ϕ_i shown in Eq. (9) into Eq. (7) gives

$$f_i = \O_i \frac{\eta_{th}}{\delta_{th}} \quad (10)$$

Also, substituting the definition of ϕ_i shown in Eq. (9) and $\sigma_i = \delta_i / 2.57$ (based on the maximum uncertainty for parameter i being in the 99th percentile) into Eq. (8) gives

$$\sigma_{th} = \frac{\eta_{th}}{2.57} \sqrt{\sum_i \O_i{}^2} \quad (11)$$

An advantage of using ϕ_i is that this term is less complex than the partial derivatives enabling δ_{th}, f_i, and σ_{th} to be quickly obtained from knowledge of η_{th} and the value of each ϕ_i.

Results

Table 1 shows the mass of fuel consumed (f_{cm}), the mass of water evaporated (Δm_{water}), the change in water temperature (ΔT), and mass of charcoal remaining (m_c) at the end of each test for the basic stove, stove with skirt, stove with grate, and stove with both a skirt and grate.

As expected, f_{cm} for each test varied significantly. The basic design used the most wood, and the least wood was consumed when the skirt and grate/skirt were used. f_{cm} for both configurations that included skirts was statistically less (99% confidence) than the basic stove. Since f_{cm} for the grate configuration was also significantly greater (90% confidence) than the skirt and significantly greater (95% confidence) than the grate/skirt configuration, this showed that the simple skirt significantly reduced fuel consumption.

The amount of water vaporized and the change in water temperature were very similar among all configurations with a maximum difference in water vaporized of 4.3 g (approximately 20 g of water was vaporized in each test) and a maximum difference in temperature changes of 0.82 K (each ΔT was approximately 70 K). This was expected since the initial water temperature for all runs was similar and the boiling temperature varied only slightly among testing days due to the slight variation in atmospheric pressure. Values of ΔT were consistent because the initial water temperature was easily controlled while the other three measured parameters (f_c, Δm_{water}, m_c) could not be directly controlled. On the other hand, the mass of the remaining charcoal varied among each type of modified cookstove. The average for each configuration ranged from 32.4 g to 52.0 g, with the grate and grate/skirt showing

Table 1
Summary of measured data for each cookstove configuration.

	f_{cm} (g)	Δm_{water} (g)	ΔT (K)	m_c (g)
Basic stove (n = 9)				
Average	566.6	19.5	70.4	52.0
Std dev	89.7	4.8	1.2	7.3
Std dev/average	0.16	0.25	0.02	0.14
Skirt (n = 9)				
Average	385.7	22.0	70.5	43.0
Std dev	24.0	4.3	1.3	8.3
Std dev/average	0.06	0.20	0.02	0.19
Grate (n = 5)				
Average	502.0	18.9	70.7	37.8
Std dev	106.9	3.5	2.5	9.8
Std dev/average	0.21	0.19	0.04	0.26
Skirt and grate (n = 5)				
Average	366.0	23.2	69.9	37.4
Std dev	42.7	6.6	1.4	4.4
Std dev/average	0.12	0.28	0.02	0.12

the least amount of charcoal. The basic cookstove showed significantly more charcoal formation (95% confidence) compared to all configurations with a skirt and/or grate. This finding suggests that the grate and/or skirt can be effective for reducing charcoal.

After each experiment, η_{th} was calculated using Eqs. (1)–(5) Then, ϕ_i was evaluated for each x_i parameter and subsequently δ_{th}, f_i, and σ_{th} were calculated using Eqs. (9)–(11). According to the definition of ϕ_i shown in Eq. (9), δ_i is required to evaluate ϕ_i. Table 2 shows δ_i for each key parameter x_i in Eqs. (2)–(5), literature values for some x_i, and the source for each δ_i. It should be noted that $\delta_{\Delta T}$ is twice the uncertainty of the thermocouple used because the term is derived from two temperatures subtracted from each other. Similarly, f_{cm} and Δm_{water} are twice the uncertainty of the measurement scale because these parameters are derived from two mass values subtracted from each other. Where literature values were used, the ratio of δ_i to the literature value ranged from about 0.01 to 0.10. Thus, some parameters can potentially have more impact on uncertainty contributions than other parameters.

Of particular interest was the quantification of δ_i for both values of LHV. The LHV of an individual species of wood can vary from tree to tree and by location within the tree. Values found in literature for Douglas fir range from 19.5 MJ/kg (Jetter and Kariher, 2009) to 21.1 MJ/kg (Kuhns and Schmidt, 2016). Using the average of these values as the value of the wood burned in this study, the maximum variance is 0.8 MJ/kg or about 4% of the value. Additionally, the values within a single tree can also vary significantly. If the lower heating value of wood used in cookstove combustion is bounded by the lower heating values of the stem (i.e. trunk) and the branches, using data from Singh and Kostecky, the average stem LHV was 19.122 for the softwoods and 18.396 hardwoods studied and the average branch LHV was 20.649 and 19.545 (Singh and Kostecky, 1986). Using the average of stem and branch LHV values as the value of the burned wood, this would give a maximum variance of $\pm 4\%$ of the value for softwoods and $\pm 3\%$ for the hardwoods. On the other hand, measurements of the LHV (such as using a bomb calorimeter) for processed fuels can lead to a very low δ_i.

Even more difficult is identifying δ_i and the literature value of LHV of the charcoal remaining from the wood as these values can vary from wood species to species and there is very little data available at that level of specificity. Taylor showed significant variance (values ranged from 22.6 MJ/kg to 31.0 MJ/kg) from the WBT's currently assumed (in the absence of user defined data) char LHV value of 29.5 MJ/kg for all wood-derived char (Taylor, 2009; Bailis et al., 2014). It is important to have a value assumed for the case where a researcher is for some reason unable to get the data necessary, and so it is also important to know how much variance may be added by using this assumption. It should be noted that researchers can use various methods (such as bomb calorimetry) to measure LHV and thereby decrease the error significantly from what is used in this study.

Eqs. (12)–(18) shows ϕ_i for all x_i parameters in Table 2 except for Cp, $m_{water,i}$, $H_{vap,Pamb}$, T_{amb}, and T_{boil}. The ϕ_i for these parameters are not shown since the sum of the fractional contribution (f_i) of each of these parameters to δ_{th} accounted for less than 1% in the experimental studies.

$$\emptyset_{LHV_{wood}} = \frac{\delta_{LHV\,wood}}{LHV_{wood}} \cdot \left[\frac{1}{1 - \left(\frac{m_c}{f_c}\right)\left(\frac{1}{1-MC(1+y)}\right)\left(\frac{LHV_c}{LHV_{wood}}\right)} \right] = \frac{\delta_{LHV\,water}}{LHV_{wood}} \cdot \left[mod_{LHV_{wood}} \right] \tag{12}$$

$$\emptyset_{\Delta T} = \frac{\delta_{\Delta T}}{\Delta T} \cdot \left[\frac{1}{1 + \left(\frac{\Delta m_{water}}{m_{water,i}}\right)\left(\frac{\Delta h_{H2O,fg}}{C_p * \Delta T}\right)} \right] = \frac{\delta_{\Delta T}}{\Delta T} \cdot \left[mod_{\Delta T} \right] \tag{13}$$

$$\emptyset_{MC} = \frac{\delta_{MC}}{MC} \cdot \left[\frac{1}{\frac{1}{MC(1+y)}\left[1 - \left(\frac{m_c}{f_{cd}}\right)\left(\frac{LHV_c}{LHV_{wood}}\right)\right] - 1} \right] = \frac{\delta_{MC}}{MC} \cdot \left[mod_{MC} \right] \tag{14}$$

$$\emptyset_{LHV_c} = \frac{\delta_{LHVc}}{LHV_c} \cdot \left[\frac{1}{\frac{1-MC(1+y)}{\left(\frac{m_c}{f_{cd}}\right)\left(\frac{LHV_c}{LHV_{wood}}\right)} - 1} \right] = \frac{\delta_{LHVc}}{LHV_c} \cdot \left[mod_{LHV_c} \right] \tag{15}$$

$$\emptyset_{m_c} = \frac{\delta_{m_c}}{m_c} \cdot \left[\frac{1}{\frac{1-MC(1+y)}{\left(\frac{m_c}{f_{cd}}\right)\left(\frac{LHV_c}{LHV_{wood}}\right)} - 1} \right] = \frac{\delta_{m_c}}{m_c} \cdot \left[mod_{m_c} \right] \tag{16}$$

Table 2
Uncertainty estimates of all measured and input parameters of η_{th} (Eqs. (1)–(5)).
Starred values indicate that the value is twice that of the instrument because it is a calculated difference.

x_i	Value	δ_i	Units	Source
Cp	4.186	0.0042	kJ/kg/K	Specific heat of water http://www.nist.gov/srd/upload/jpcrd38200921p.pdf
$m_{water,i}$		0.5	g	Salter® scale. http://www.salterusa.com/salter_us/catalog-us/kitchen-scales/aquatronicr-high-capacity-scale-with-touchless-tare.html
ΔT		1.0*	K	K-type thermocouple after calibration.
$H_{vap,Pamb}$	2260	0.4	kJ/kg	Heat of vaporization of saturated water at ambient pressure which is assumed to be 1 atm. http://www.iapws.org/relguide/Advise1.pdf
Δm_{water}		1.0*	g	Salter® scale. http://www.salterusa.com/salter_us/catalog-us/kitchen-scales/aquatronicr-high-capacity-scale-with-touchless-tare.html
f_{cm}		1.0*	g	Salter® scale. http://www.salterusa.com/salter_us/catalog-us/kitchen-scales/aquatronicr-high-capacity-scale-with-touchless-tare.html.
MC		2.5	%	General Tools® moisture meter http://www.generaltools.com/MMD4E--Pin-type-LCD-Moisture-Meter_p_636.html
LHV_{water}	19,314	965	kJ/kg	Variation in literature shows approximately 5%
LHV_c	29,500	2950	kJ/kg	The WBT worksheet assumes this value in the absence of other data. Assumed 10% uncertainty since data was not readily available and this value can vary significantly across tree species, though it can be determined with good accuracy through several methods as discussed in the body of this work.
m_c		0.5	g	Salter® scale. http://www.salterusa.com/salter_us/catalog-us/kitchen-scales/aquatronicr-high-capacity-scale-with-touchless-tare.html
T_{amb}		0.5	K	K-type thermocouple after calibration.
T_{boil}		NA	K	Calculated boiling temperatures

$$\O_{f_{cd}} = \frac{\delta_{f_{cd}}}{f_{cd}} \cdot \left[\frac{1}{1 - \frac{\left(\frac{LHV_c}{LHV_{wood}}\right)\left(\frac{m_c}{f_{cd}}\right)}{1 - MC(1+y)}} \right] = \frac{\delta_{f_{cd}}}{f_{cd}} \cdot [mod_{f_{cd}}] \tag{17}$$

$$\O_{\Delta m_w} = \frac{\delta_{\Delta m_{water}}}{\Delta m_{water}} \cdot \left[\frac{1}{1 + \left(\frac{m_{water,i}}{\Delta m_{water}}\right)\left(\frac{C_p * \Delta T}{\Delta h_{H2O,fg}}\right)} \right] = \frac{\delta_{\Delta m_{water}}}{\Delta m_{water}} \cdot [mod_{\Delta m_{water}}] \tag{18}$$

As seen, each ϕ_i has two essential elements. The first element is a ratio between the parameter uncertainty (δ_i) and the corresponding value of the parameter. The second element is a modulation factor that may amplify or attenuate ϕ_i and can lead to some experimental guidelines as discussed later. When looking at the modularity terms in Eqs. (12)–(18), the modularity terms in Eqs. (12) and (14)–(17) will always amplify ϕ_i and the modularity terms in Eqs. (13) and (18) will always attenuate ϕ_i.

Fig. 2 shows the relationship between δ_{th} and η_{th} where the units are % efficiency. The highest η_{th} of 15% corresponds to a δ_{th} of 2.18% (which is 15% of η_{th}), and the lowest η_{th} of 6.2% corresponds to a δ_{th} of 0.76% (which is 12% of η_{th}). Interestingly, δ_{th} has an upward linear correlation with η_{th} with an intercept at the origin. The reason for the linear correlation is outlined in the Discussion section. It should also be noted that there is no cookstove configuration involving a skirt that has a thermal efficiency below 11%. All cookstoves with skirts showed η_{th} ranging from 11.7% to 14.6%. Of the tests with a cookstove configuration lacking a skirt, there is one (grate only) with η_{th} of 15%. This point has been determined to be an outlier (it is well outside the 99% confidence interval of the other values). However, this outlier is still consistent with the linear relationship. None of the other tests without a skirt reached a η_{th} greater than 10.3%. The η_{th} for both configurations with a skirt were significantly greater (99% confidence) than the configurations without a skirt. The average efficiencies (standard deviation) for the basic, skirt, grate, and both configurations were 8.9% (1.8%), 12.8% (0.8%), 8.6% (1.5%), and 13% (1.4%) respectively. This again shows that the skirt is critical to increasing the thermal efficiency by ensuring that more of the thermal energy released by the fuel is transferred to the water in the pot. This is consistent with the findings in Table 1 where less wood was used with a skirt.

Fig. 3 shows f_i for the top four parameters contributing to δ_{th} for each cookstove configuration. Each bar represents the average f_i for all studies involving a given cookstove configuration, with the error bars representing one standard deviation. Interestingly, the average f_i associated with LHV_{wood} was around 0.44 (44%) for all configurations. Thus, a more accurate value of LHV_{wood} would reduce δ_{th}. The average f_i for ΔT was near 0.10 (10%) for all cookstove configurations. The average f_i for MC was near 0.26 (26%) and the average f_i for LHV_c was around 0.14 (14%) for all cookstove configurations. For each cookstove configuration, the top four parameters accounted for approximately 93% of δ_{th}.

It is interesting to note that for each cookstove configuration, the f_i values appear to be independent of the cookstove configuration. Based on the four parameters contributing the most to δ_{th}, the independence is expected since LHV_{wood} and LHV_c are based on literature values and ΔT and MC are controlled variables. Also of interest is that when f_i for ΔT increases or decreases, the f_i contribution for LHV_c changes in the opposite direction. In general, more accurate LHV values, thermocouples, and moisture analysis than was used in this study would be beneficial.

Fig. 4 shows σ_{th} versus η_{th} for all studies (diamonds) where a linear correlation is again observed. Regression results in $\sigma_{th} = 0.029 * \eta_{th}$ with an R^2 value of 0.96. The 95% confidence interval of the linear fit (dotted lines) is also shown. The confidence interval demonstrates a very tight fit around the line such that the line is a very accurate representation of σ_{th} versus η_{th} for this study.

In cookstove studies, the standard deviation associated with a group of experiments is often reported. The difficulty of only reporting the standard deviation is that it does not necessarily include all uncertainties (a differing LHV value based on different literature sources, for instance, would result in a bias in the observed values that could not be accounted for with a simple standard deviation of the data) although it does include error associated with testing conditions that are not explicitly included in the calculation of σ_{th}. Testing conditions would include parameters such as wind speed, ambient temperature, atmospheric pressure, and relative humidity, which would require further investigation as to their effects. Thus, comparison of σ_{th} using propagation of uncertainties in measurements and input data with the uncertainty calculated using the standard deviations of the results of a group of experiments is informative. Therefore, Fig. 5 includes the average η_{th} and associated standard deviation (symbols) of the group of experiments for each cookstove configuration with a line representing the regression curve from Fig. 4. The average η_{th} (and σ) for the basic stove, skirt, grate, and both grate and skirt configurations were 8.9 (±1.8), 12.8 (±0.8), 9.7 (±2.9), and 13 (±1.4) % respectively. The line was extrapolated to 40% assuming that the linear relationship between σ_{th} and η_{th} was still

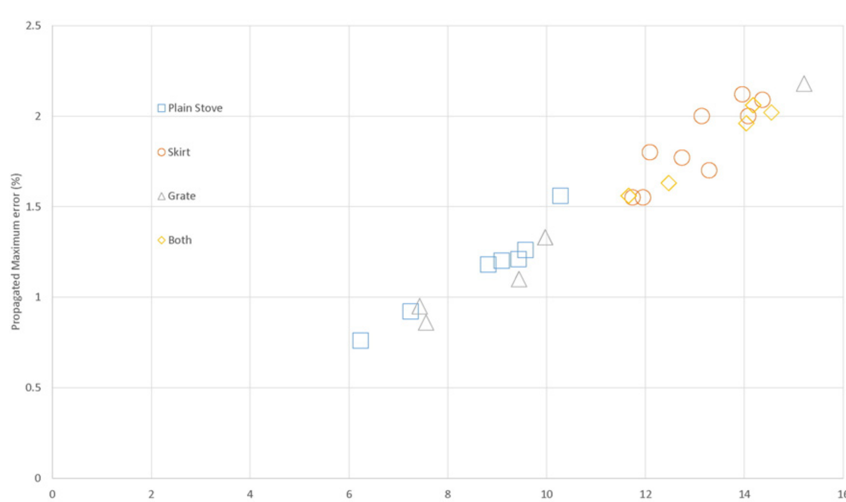

Fig. 2. Propagated Maximum Error (δ_{th}) vs. η_{th}. Both axes are in units of % efficiency. The squares, triangles, circles, and diamonds represent data from the basic cookstove, the cookstove with a grate added, the cookstove with a skirt added, and the cookstove with both a grate and a skirt added, respectively.

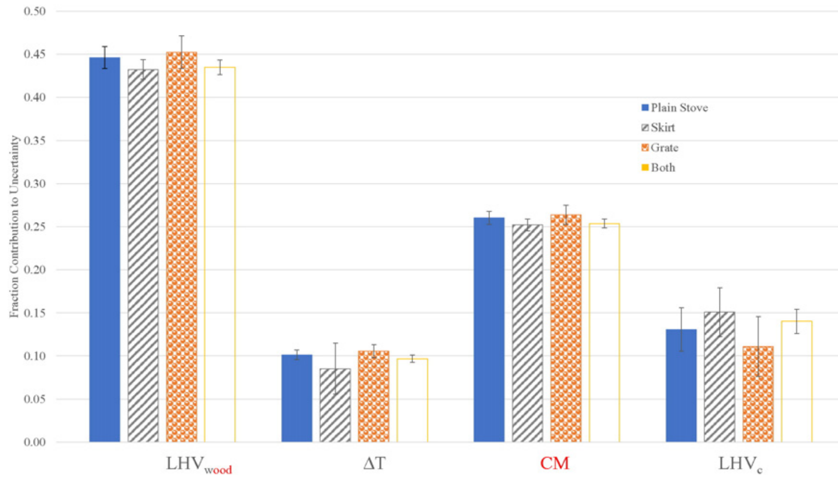

Fig. 3. Fraction contribution to uncertainty (f_i). The figure shows f_i (Eq. (10)) for the top four most contributing parameters in Eqs. (1)–(5) The solid, slanted lined, circle filled, and empty columns represent data from the basic cookstove, the cookstove with a grate added, the cookstove with a skirt added, and the cookstove with both a grate and a skirt added, respectively.

valid over this extended range. Based on the four parameters above that contribute the most to the propagated uncertainty, the assumption of linearity over this range is likely valid if the same equipment were used in all experiments. Further validation of the linearity is discussed below. Additionally, the extremely consistent data and tight confidence interval shown in Fig. 4 suggest that this extrapolation is also valid.

As can be seen in Fig. 5, the averaged results for each cookstove configuration give a higher standard deviation than can be accounted for by just σ_{th}. This result clearly indicates that in the low η_{th} range, standard deviations associated with η_{th} are dominated by variability in ambient conditions (e.g. wind speed, humidity) and testing procedures (e.g. method and rate of feeding wood, using unprocessed versus processed fuels) that are not directly part of the efficiency equation and are much more difficult to control. However, measurement uncertainty can potentially become more important as η_{th} increases as shown in Fig. 5. Thus, it would be beneficial when comparing cookstoves to address the contributions of measurement and input data uncertainties. In some instances, measurement uncertainty (e.g. temperature and percent moisture) can depend upon the equipment used. In contrast, literature data uncertainty due to the LHV values depends upon the literature value used and the associated uncertainty of the value. Thus, cookstove results should report all input data (e.g. LHV_{wood}).

Discussion

Analyzing the modulation factors in Eqs. (12)–(18) leads to some insight into the behavior of the uncertainty associated with these parameters. For example, Eq. (12) indicates that decreasing the moisture content (*MC*) of the wood will increase the denominator of the modulation factor and therefore reduce the LHV_{wood} contribution to δ_{th}. A low ratio of charcoal produced to fuel burned (m_c/f_{cm}) will also reduce the LHV_{wood} contribution to δ_{th}, though this is a characteristic of the stove and cannot be changed through changes in the protocol. Wood with higher LHV_{wood} will also lead to lower uncertainty. Thus, studies using dry, hard woods will generally experience less uncertainty than studies using more moist woods and/or soft woods. However, it is important to use wood that is appropriate for the stove design and to know how that will affect uncertainty.

Interestingly, Eq. (13) shows that bringing the ratio of Δm_w to m_{wi} to its maximum value of unity would be the protocol change that would

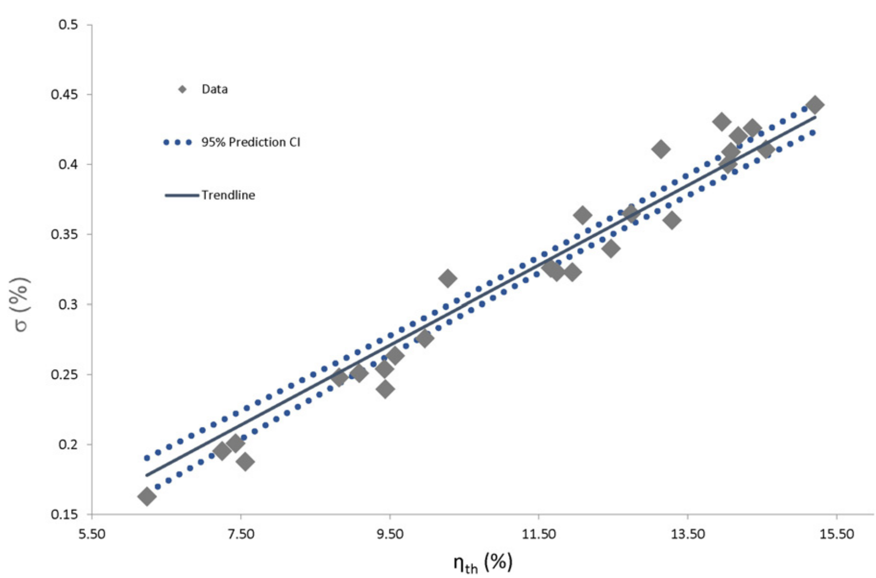

Fig. 4. Propagated standard deviation (σ_{th}) vs. η_{th}. Both axes are in units of % efficiency. The data for all cookstove configurations is shown as diamonds, with a solid trendline for the fit. A 95% confidence interval of the linear fit is also shown as a dotted line.

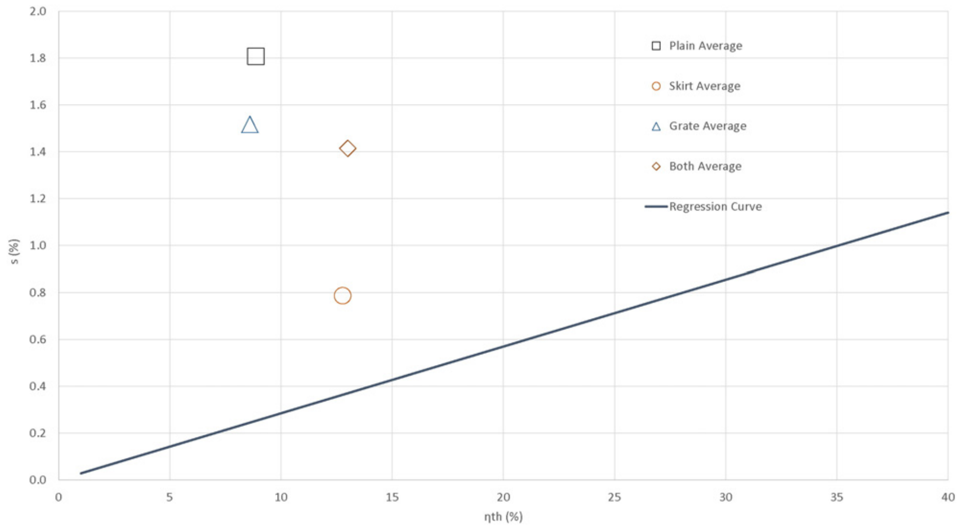

Fig. 5. Standard deviation (σ) vs. η_{th}. Both axes are in units of % efficiency. The unfilled squares, triangles, circles, and diamonds represent standard deviations associated with each group of experiments for the basic cookstove, the cookstove with a grate added, the cookstove with a skirt added, and the cookstove with both a grate and a skirt added, respectively. The solid line represents the propagated standard deviation regressed from Fig. 4 and is extended to 40% efficiency.

most reduce the uncertainty contribution from ΔT. This is unrealistic since boiling to completion takes a significant amount of time. If 15% of the water boiled ($\Delta m_{water}/m_{water,i} = 0.15$), the ΔT uncertainty contribution would be 50% of the contribution compared to when no water is boiled, and if 50% of the water is boiled, the contribution of the uncertainty in ΔT decreases to 29%. This calculation was based on a ΔT of 80 K, which is a typical value for cookstove tests. However, implementing this strategy for reducing the uncertainty in η_{th} would dramatically increase the time required to perform a test which would likely not be practical. Additionally, a higher ΔT also leads to a lower contribution such that starting with a colder water and approaching boiling could be another option for reducing the uncertainty contribution from ΔT. However, there are physical limitations since ΔT is bound by realistic operating conditions between ambient temperature and boiling. It is therefore, best to control the uncertainty due to temperature measurements by either calibrating thermocouples or using more accurate devices to measure temperature such as an RTD.

Eqs. (14)–(17) also indicate that low MC and low m_c/f_{cm} will minimize the contribution of the uncertainty in MC and LHV_c to the uncertainty in η_{th}. Thus, similar to the findings in Eq. (12), dry wood would be the best to use to reduce measurement uncertainty. However, dry wood is often not found in the field and some stoves do not perform as well with dry wood. In situations where moist wood is needed, it would be important to pay more particular attention to minimizing measurement uncertainty of moisture content. Additionally, minimizing the formation of charcoal by increasing airflow would be beneficial.

Eq. (18) shows similar design guidelines found in Eq. (13). For instance, a large ΔT can help mitigate the uncertainty associated with Δm_{water}. However, Eq. (18) is not affected by the ratio of $m_{water,i}$ to Δm_{water}, but rather is affected individually by $m_{water,i}$ and Δm_{water}. Both a large $m_{water,i}$ and Δm_{water} will mitigate this uncertainty. This would imply using the largest amount of water and boiling it to completion. However, using a large amount of water may decrease the relevancy of the results as the stove should be tested under conditions as similar to field use as possible. Considering that f_i of Δm_{water} is very small (and therefore $\phi_{\Delta mwater}$ is very small) and the possibility of less useful results this method of reducing uncertainty is not worth the time and cost for most studies.

Another interesting result is that the summation of each ϕ_i explains the linearity of the uncertainty as shown in Figs. 2 and 4. In Eqs. (12)–(18), all of the parameters in the modulation terms except m_c/f_{cm} can be controlled and remain the same between experimental studies, even if cookstove configurations change significantly as was done in this study. Additionally, m_c/f_{cm} is usually less than 0.1. Focusing on the four most significant parameters (Eqs. (12)–(15)) shown in Fig. 3, since f_i for each parameter was constant, then the ϕ_i was also constant according to Eq. (10). Therefore, Eq. (9) shows that ratio of δ_{th}/η_{th} is constant which is consistent with Fig. 2.

Similarly, Eq. (11) also shows then that ratio of σ_{th}/η_{th} is constant which is consistent with Fig. 4.

It should be noted that the actual values of the contributions reported in this study are specific to this set of experimental parameters, equipment, and testing protocols. However, Eqs. (12)–(18) can be readily used in any cookstove study that uses the same definition for η_{th} to calculate δ_{th}, f_i, and σ_{th} associated with measurement and input data at any given η_{th}.

Conclusions

This study showed how to quickly determine propagated values of δ_{th} and σ_{th}, as well f_i, from a given η_{th} based on uncertainties associated with measured and input data associated with the efficiency equation. This allows for an understanding of how significant δ_{th} and σ_{th} are in comparison to η_{th}. Additionally, this analysis is important because it helps assess how these values can compare to population standard deviations for a set of experiments and provides some guidance as to the importance of measurement and input value uncertainties. As shown, δ_{th} becomes increasingly important as η_{th} increases. Thus, rigorous assessment of the relative impact of all measured and input parameters on cookstove performance metrics, such as η_{th}, is critical. In addition, the fractional contribution (f_i) of each parameter to δ_{th} indicates which parameters are important to focus on for reducing measurement and input value uncertainties. For this study LHV_{water}, LHV_{ch}, ΔT, and MC were the critical parameters such that more accurate LHV values, thermocouples, and moisture analysis would be beneficial. It should also be noted that, while not part of this study, the effects of error in separating wood and char values can be very important. These effects can be found in Taylor's work, where it was suggested that it is better to err on the side of counting char as fuel rather than the other way around (Taylor, 2009).

Another valuable aspect of this study is that it provided guidance on experimental procedures to minimize measurement and input data uncertainty contributions to η_{th}. The results of this study indicate that reducing the moisture content of the wood, reducing the ratio of the mass of the char to the mass of wood, using wood with a large heating value, boiling off a reasonable fraction of the water (e.g. 15%) in the pot, and starting with relatively cold water will reduce the uncertainty in the measured thermal efficiency. However, these recommendations may have large costs associated with them (e.g. time to boil water), may have physical limitations (e.g. ΔT is bound by the freezing and boiling temperatures), and/or may be limited by the operational guidelines of the cookstove (e.g. moisture content, fuel type).

On the other hand, the δ_i associated with each parameter x_i is much easier to decrease. For LHV values, as previously stated it may not be possible to significantly reduce the uncertainty in wood LHV values when using cut wood unless a more processed fuel such as wood pellets is used. However, the LHV of the char may be significantly easier to estimate as the char can be easily ground into a powder and either measured by bomb calorimetry or estimated through various means (e.g. by analyzing the chemical makeup of the char and Thornton's rule or proximate analysis). By comparison with LHV values, thermocouples are much easier to improve through calibration. The WBT protocol suggests a minimum accuracy of ± 0.5 °C, which improves the uncertainty from thermocouples compared to uncalibrated thermocouples which can be on the order of ± 2.0 °C based on manufacturer specifications. Another important observation is that moisture content (MC) can be much more accurately obtained through the oven-drying method, which suggests that the moisture meter may not be the optimal choice although the meter is much simpler and quicker to use.

It should be noted that the above conclusions address issues associated with parameters directly expressed in the η_{th} definition (Eqs. (1)–(5)). The above method can be applied to any study to assess the impact of measurement uncertainty using reasonable values for that study. It is important to characterize and report measurement uncertainty associated with the parameters to provide insights on which measurements contribute the greatest amount to uncertainty and the degree to which measurement error contributes to overall uncertainty which also includes effects of indirect parameters (such as shape of fuel, wind speed, humidity). Particularly, reporting the LHV value and its associated uncertainty is highly valuable. Finally, it is beneficial that all literature data and test conditions be reported to enable better comparisons between cookstoves.

Acknowledgements

Appreciation is extended to Jae Cho, Kendall Thacker, and McCall Barger for their assistance in performing the experiments used in this analysis.

References

Abeliotis K, Pakula C. Reducing health impacts of biomass burning for cooking — the need for cookstove performance testing. Energy Effic 2013;6(3):585–94.
Agenbroad JN. A simplified model for understanding natural convection driven biomass cooking stoves; 2010.
Andreatta D, Wohlgemuth A. An investigation of skirts; 2010.
Bailis P, Ogle D, Maccarty N, From D. The water boiling test (WBT); 2014 [[cited 2014 Aug 22];2(March 2014). Available from: http://citeseerx.ist.psu.edu/viewdoc/summary?doi=10.1.1.406.1467].
Baldwin SF. Biomass stoves, engineering design, development and dissemination; 1987.
Bethea RM, Rhinehart RR. Applied engineering statistics. NY: Marcel Dekker; 1991.
Bond TC, Doherty SJ, Fahey DW, Forster PM, Berntsen T, Deangelo BJ, et al. Bounding the role of black carbon in the climate system: a scientific assessment. J Geophys Res Atmos 2013;118(11):5380–552.
Chowdhury Z. Quantification of indoor air pollution from using cookstoves and estimation of its health effects on adult women in northwest Bangladesh. Aerosol Air Qual Res 2012;12:463–75.
Hawley B, Volckens J. Proinflammatory effects of cookstove emissions on human bronchial epithelial cells. Indoor Air 2013;23(1):4–13.
Jetter JJ, Kariher P. Solid-fuel household cook stoves: characterization of performance and emissions. Biomass and bioenergy [internet], 33(2). Elsevier Ltd; 2009. p. 294–305. http://dx.doi.org/10.1016/j.biombioe.2008.05.014 [Available from:].
Jetter J, Zhao Y, Smith KR, Khan B, Yelverton T, Decarlo P, et al. Pollutant emissions and energy efficiency under controlled conditions for household biomass cookstoves and implications for metrics useful in setting international test standards. Environ Sci Technol 2012;46(19):10827–34.
Kshirsagar MP, Kalamkar VR. A comprehensive review on biomass cookstoves and a systematic approach for modern cookstove design. Renew Sustain Energy Rev 2014;30(1):580–603.
Kuhns M, Schmidt T. Wood heating [internet]; 2016 [Available from: https://forestry.usu.edu/htm/forest-products/wood-heating].
MacCarty NA, Bryden KM. Modeling of household biomass cookstoves: a review. Energy Sustain Dev [Internet]. Int Energy Initiat 2015;26:1–13. http://dx.doi.org/10.1016/j.esd.2015.02.001. (Available from:).
Manoj K, Sachin K, Tyagi SK. Design, development and technological advancement in the biomass cookstoves: a review. Renew Sustain Energy Rev 2013;26(1):265–85.
Mueller V, Pfaff A, Peabody J, Liu YP, Smith KR. Demonstrating bias and improved inference for stoves' health benefits. Int J Epidemiol 2011;40(6):1643–51.
Poudyal M, Cranney A, Jones MR, Lewis RS. Impact of co-firing a traditional Peruvian biomass cookstove with biogas on emissions and combustion efficiency. IEEE GHTC; 2015. p. 1–8.
Singh T, Kostecky MM. Calorific value variations in components of 10 Canadian tree species. Can J For Res 1986;16(1984):1378–81. [Available from: http://www.nrcresearchpress.com/doi/abs/10.1139/x86-245].
Taylor RPI. The uses of laboratory testing of biomass cookstoves and the shortcomings of the dominant U.S. protocol; 2009.
Wohlgemuth A, Mazumder S, Andreatta D. Computational heat transfer analysis of the effect of skirts on the performance of third-world cookstoves. J Therm Sci Eng Appl 2009;1(4):041001.
Zube DJ. Heat transfer efficiency biomass cookstoves (Zube MS Thesis) Colorado State University; 2010.